The Two Actin-Binding Regions on the Myosin Heads of Cardiac Muscle†

Takayuki Miyanishi,*,‡,§ Takashi Ishikawa,||,⊥ Toshihisa Hayashibara,§ Tetsuo Maita,§ and Takeyuki Wakabayashi||,#

Faculty of Environmental Studies, Nagasaki University, Nagasaki 852-8521, Japan, Department of Biochemistry, Nagasaki University School of Medicine, Nagasaki 852-8523, Japan, and Department of Physics, Graduate School of Science, University of Tokyo, Hongo, Tokyo 113-0033, Japan

Received September 24, 2001; Revised Manuscript Received January 22, 2002

ABSTRACT: In the presence of myosin S1 or myosin heads, actin filaments tend to form bundles. The biological meaning of the bundling of actin filaments has been unclear. In this study, we found that the cardiac myosin heads can form the bundles of actin filaments more rapidly than can skeletal S1, as monitored by light scattering and electron microscopy. Moreover, the actin bundles formed by cardiac S1 were found to be more stable against mechanical agitation. The distance between actin filaments in the bundles was ~20 nm, which is comparable to the length of a myosin head and two actin molecules. This suggests the direct binding of S1 tails to the adjacent actin filament. The "essential" light chain of cardiac myosin could be cross-linked to the actin molecule in the bundle. When monomeric actin molecules were added to the bundle, the bundles could be dispersed into individual filaments. The three-dimensional structure of the dispersed actin filaments was reconstructed from electron cryo-microscopic images of the single actin filaments dispersed by monomer actin. We were able to demonstrate that cardiac myosin heads bind to two actin molecules: one actin molecule at the conventional actin-binding region and the other at the essential light-chain-binding region. This capability of cardiac myosin heads to bind two actin molecules is discussed in view of lower ATPase activity and slower shortening velocity than those of skeletal ones.

The actin−myosin interaction is the basis for many biological phenomena. Myosin has two types of light chains, i.e., the "essential" (alkali) light chains and the "regulatory" light chains (*1*). In skeletal muscle, the actin−myosin interaction depends on the presence of essential light chains. The myosin heads with essential light chain (ELC)[1] 1 can bind actin more tightly than the head with ELC 2 which has the same amino acid sequence except for the amino-terminal 41 residues of ELC 1 (*2*−*4*). In the presence of an excessive amount of rabbit skeletal myosin subfragment-1 (S1) over actin, the bundling of actin filaments was facilitated, with the interfilament distance being ~18 nm (*5*). Ando described this phenomenon as hyper-opalescence. When using chicken skeletal myosin S1, we confirmed the hyper-opalescent type bundle of actin filaments under the same conditions, i.e., at a molar ratio of 1:1 S1 to actin (*6*). We further found that myosin S1 with ELC 1 was capable of forming a bundle while that with ELC 2 was much less effective (*6*). This is consistent with the observation that the amino-terminal region of ELC 1 on myosin can interact directly with the actin molecule while that of ELC 2 of myosin cannot (*2, 4*). In the case of either rabbit or chicken skeletal muscle myosin S1, the formed bundle was rather unstable, and shaking the solution of bundles resulted in a decrease of light scattering; i.e., the bundles were dispersed (*6*). The biological meaning of actin bundling capability of the muscle myosin head has been unclear and not well understood. In this study, we found that myosin S1 from cardiac muscle can form stable bundles, and it was possible to reconstruct a three-dimensional structure of the acto−S1 complex. We demonstrated that cardiac myosin head containing ELC can bind two actin molecules at a time at two different regions, the conventional actin-binding region and the ELC-binding region. This capability is discussed in relation to the cardiac muscle characteristic of lower ATP-splitting rate and shortening velocity than skeletal muscle.

EXPERIMENTAL PROCEDURES

Proteins. Skeletal myosin was prepared from chicken breast muscle as elsewhere described (*7*). Cardiac myosin was prepared from chicken ventricle muscle as elsewhere described (*8*). S1 was obtained by α-chymotryptic digestion (1:200, w/w) of myosin filament by the method of Weeds and Taylor (*9*), and further purified by Cellulofine DEAE A500 (Chisso, Tokyo, Japan) column chromatography. Only

† This work was supported in part by the Ministry of Education, Culture, Sports, Science and Technology of Japan.

* Correspondence should be addressed to this author at the Faculty of Environmental Studies, Nagasaki University, Nagasaki 852-8521, Japan. Tel: +81-95-843-2186; Fax: +81-95-843-2182; Email: miyanish@net.nagasaki-u.ac.jp.

‡ Faculty of Environmental Studies, Nagasaki University.

§ Nagasaki University School of Medicine.

|| University of Tokyo.

⊥ Present address: Laboratory of Structural Biology Research, NIAMS, NIH, Bethesda, MD.

Present address: Department of Biosciences, School of Science and Engineering, Teikyo University, Toyosatodai 1−1, Utsunomiya 320−8551, Japan.

[1] Abbreviations: BSA, bovine serum albumin; EDC, 1-(3-dimethylaminopropyl)-3-ethylcarbodiimide; ELC, essential light chain of muscle myosin; DACM, *N*-[7-(dimethylamino)-4-methylcoumarin-3-yl]maleimide; IAF, iodoacetamidofluorescein; IATR, tetramethylrhodamine iodoacetamide; MBS, 3-maleimidobenzoic acid *N*-hydroxysuccinimide ester; S1, subfragment-1 of myosin.

10.1021/bi0118355 CCC: $22.00
Published on Web 04/06/2002

the peak fraction of the chromatography was used in this work, or after dialyzing against an appropriate buffer when necessary. Cardiac ELC was isolated (*10*) and exchanged with that in skeletal S1 in the presence of ammonium chloride (*11*). Actin was prepared according to Spudich and Watt (*12*), and was made nucleotide-free by passing over a resin or dialysis before use. All protein preparation was done in a low-temperature room (4 °C). Protein was determined by the Biuret method. SDS−PAGE was performed as elsewhere described (*13*).

Chemicals. All chemicals were of reagent grade.

Chemical Modification. To make S1 fluorescent, it was modified with a slight mole excess of IATR (Molecular Probes, Eugene, OR) or DACM (Dojindo, Kumamoto, Japan) at 0.1 M NaCl, 50 mM imidazole hydrochloride at pH 7 and 0 °C for 12 h as elsewhere described (*14*). The 20 μM ELC was made fluorescent by modification with 100 μM IAF (Molecular Probes) at 50 mM Tris-HCl at pH 7.8 and 0 °C, overnight. Then 30 μM actin was modified with 200 μM DACM at 0.6 M KCl, 50 mM Tris-HCl, and 1 mM $MgCl_2$ at 0 °C and pH 7.8 for 20 min. The reactions were quenched with 100 mM 2-mercaptoethanol and then washed by passing over Sephadex G-25 (Pharmacia Japan, Tokyo, Japan) or by ultracentrifugation. Nucleotide-free monomer actin (MBS-actin) was obtained by MBS (Sigma Japan, Tokyo, Japan) treatment of freshly prepared G-actin at 2 mM HEPES and 0.1 mM $CaCl_2$ at pH 7 and 0 °C for 30 min and quenched by DTT and glycine as elsewhere described (*15*), and used after ultracentrifugation to discard possible actin polymer. Cross-linking was performed with 10 mM EDC (Sigma) for 1 μM actin and with slight molar excess of S1 at 20 mM imdazole hydrochloride at pH 7 and 20 °C for 20 min, otherwise described in the text.

Fluorescence Dichroism Detection. Fluorescence dichroism detection was performed as elsewhere described (*14*) with a slight modification. When cardiac S1 was modified with IATR, fluorescent probe was incorporated mostly to the SH1 of the S1 heavy chain. A glycerinated skeletal muscle fiber was then irrigated with the fluorescent S1, which was found to bind to the actin filaments in the muscle fiber. When the muscle fiber with the fluorescent S1 was examined with a Zeiss fluorescence microscope with excitation light for the rhodamine probe polarized at 0° and 90° to the axis of the muscle fiber, fluorescence intensity from the muscle fiber depended on the angle of the polarized excitation light, which was recorded with a photomultiplier (Hamamatsu Photonics, Japan) or a CCD camera (Hitachi, Japan) attached to the microscope.

Light Scattering. The light scattering intensity of actin solution before and after adding S1 solution was monitored at 400 nm, 2 mM $MgCl_2$, and 20 mM imidazole hydrochloride at pH 7 and 25 °C using a Shimadzu RF5000 fluorospectrophotometer with a fixed slit width, light intensity and sensitivity, and with temperature regulation.

Electron Microscopy and Image Analysis. Five microliters of actin−S1 solution was applied to freshly carbon-coated grids and stained with 1% uranyl acetate, and observed with a JEM100S (JEOL) electron microscope at 80 kV. Electron cryo-microscopy and image analysis were carried out as previously described (*16*). The solution containing skeletal actin and cardiac S1 with or without MBS-actin was mounted on a holey carbon grid and plunged into a liquid ethane slush (*17*). Micrographs for the image analysis were recorded with an HF2000 electron microscope (Hitachi) with a cold field-emission gun at an accelerating voltage of 200 kV, with a nominal magnification of 30000× and ~3 μm underfocus. The electron dose was ~15 $e^-/Å^2$. Individual images of filaments were digitized with a CCD film scanner (LeafScan45, Scitex) using a step size of 5 μm. Helical reconstruction was carried out using the program developed in Medical Research Council (Cambridge) (*18*). The diffraction pattern within the first zero of the contrast transfer function (*19*) was used for reconstruction.

RESULTS

We found that cardiac myosin S1 induced bundling of actin filaments faster and the resultant bundles were more resistant to the mechanical agitation in comparison to skeletal myosin S1. Figure 1A shows the time course of light scattering increase of actin filament solution induced by adding cardiac myosin S1 in a slight excess of actin concentration. The increase was completed instantly after mixing the solution within a few seconds and remained stable even when the solution was shaken mechanically by hand or by magnetic stirrer. The light scattering increase induced by cardiac S1 was not altered by SH1 modification of the cardiac S1 heavy chain or by light-chain exchange with fluorescently labeled cardiac ELC (data not shown). Electron microscopy of an actin solution showing increased light scattering revealed that bundles were formed (Figure 2a), indicating that this increased light scattering was caused by formation of actin bundles. Typical images of neighboring actin filaments in a bundle showed antiparallel arrowheads. The space between two adjacent filaments in a bundle was ~20 nm (center-to-center). The value obtained from the negatively stained images was consistent with measurements by electron cryo-microscopy (data not shown). Whether ELC is involved in the bundle formation was examined by ELC exchange experiments. Figure 1B shows the light scattering caused by bundle formation, using skeletal myosin S1 with various ELCs. Cardiac ELC with skeletal S1 heavy chain induced light scattering increase more than 3 times faster than did skeletal ELC 1 with the same host heavy chain. Skeletal ELC 2 with skeletal S1 heavy chain did not induce any significant change in light scattering, in agreement with our previous observation (*6*). The time to reach half-maximal light scattering was estimated at 5, 600, and 2000 s for cardiac S1, skeletal S1 heavy chain with cardiac ELC, and skeletal S1 heavy chain with skeletal ECL 1, respectively. Cardiac S1 could induce actin filament bundles about 400 times faster than skeletal S1 with skeletal ELC 1 (Figure 1). Raising the pH of the bundling solution from 7 to 8 decreased the light scattering value by about 20% (data not shown).

Whether bundle formation is affected by the presence of certain salts was examined by adding NaCl or KCl to the medium. As shown in Figure 3A, NaCl and KCl had similar effects on the light scattering or the formation of actin bundles; they decreased the light scattering significantly when over 150 mM. Electron microscopy of such actin solutions showed that 200 mM NaCl can almost completely abolish formation of actin bundles (Figure 2b). On washing out the salt from such a sample on the grid before staining the sample with uranyl acetate, the actin bundles were restored, as shown in Figure 2c. The effect of salt on bundle formation,

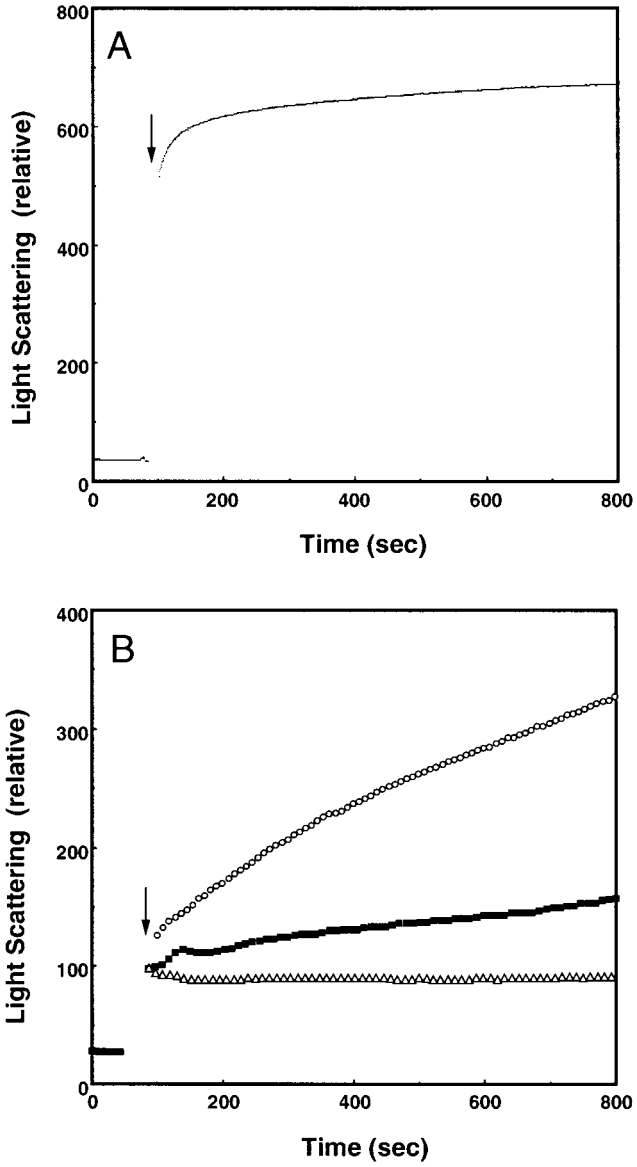

FIGURE 1: Change in light scattering from an actin filament solution observed at 400 nm by the addition of S1. (A) 1.5 μM cardiac S1 was added (at the time indicated by an arrow) to 1 μM actin solution containing 2 mM $MgCl_2$ and 20 mM imidazole hydrochloride at pH 7 and 25 °C. Light scattering was monitored at 400 nm as described under Experimental Procedures. The change in the first few seconds could not be monitored due to manual mixing of the S1 solution. (B) 1.5 μM skeletal S1 heavy chain with different essential light-chain (ELC) isoforms added at the time indicated by an arrow to 1 μM actin solution as described for (A). Open circles (top) are for S1 with cardiac myosin ELC, closed squares (middle) for S1 with skeletal myosin ELC 1, and open triangles (bottom) for S1 with skeletal myosin ELC 2.

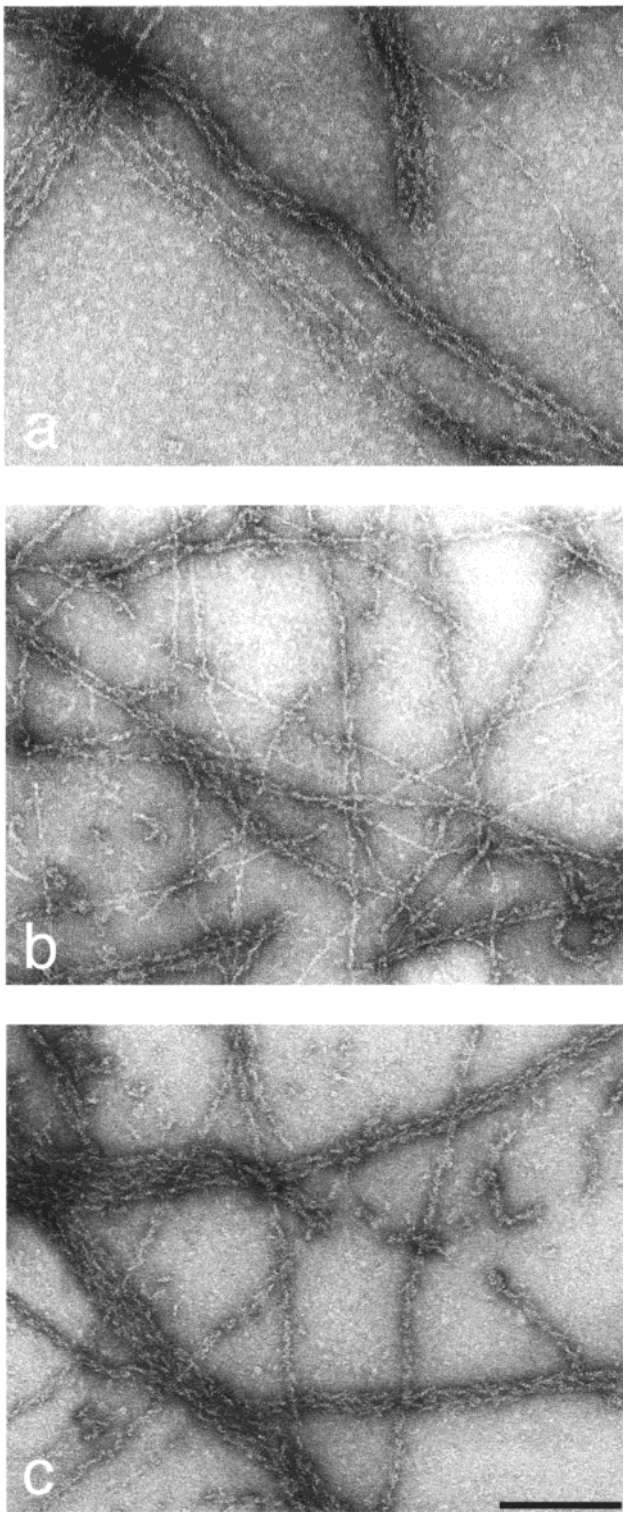

FIGURE 2: Electron micrographs of actin bundles induced by cardiac S1. Cardiac S1 was added to the actin solution as described for Figure 1, and then negatively stained and observed (a) as described under Experimental Procedures; (b) 200 mM NaCl significantly dispersed actin bundle formation; (c) antiparallel actin bundles could be observed once again after washing salt with plain buffer on the grid before the staining. Bar indicates 0.2 μm.

therefore, was shown to be reversible. We then compared the light scattering of an actin solution after addition of cardiac S1 at 0 or at 200 mM NaCl (Figure 3B). At 0 mM NaCl, the light scattering increased significantly upon increasing the amount of cardiac S1 added to the actin solution, while at 200 mM NaCl there was a small linear increase in the light scattering on increasing the amount of cardiac S1. We estimated the bundle formation induced by cardiac S1 from the difference between the two light scattering curves obtained at 0 and 200 mM NaCl. The values obtained (closed circles, Figure 3B) after such correction for the light scattering irrelevant to the bundle formation corresponded well with the calculation based on the behavior of a quadratic function of fraction (ratio) of cardiac S1 occupancy of actin molecule (dotted line, Figure 3B). Further addition of cardiac S1 in excess of a 1:1 actin stoichiometry induced no further change of the light scattering due to the bundle formation (closed circles, Figure 3B), indicating that

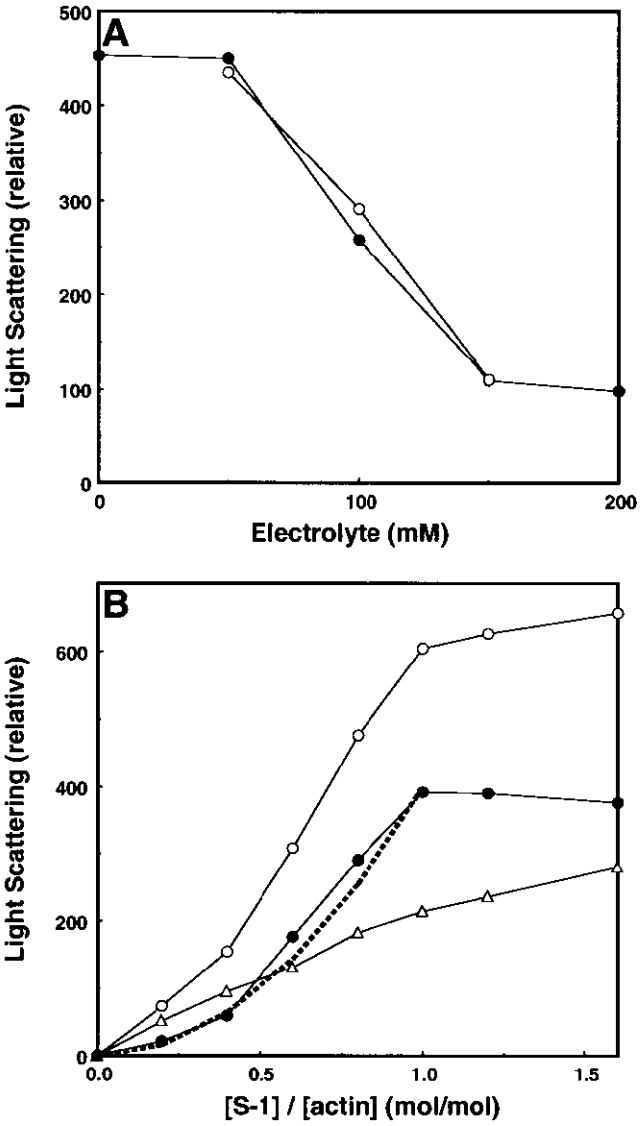

FIGURE 3: (A) Effect of electrolyte on bundle formation monitored by light scattering. 0−200 mM NaCl (closed circles) and KCl (open circles) was added to the actin solution as described for Figure 1 before adding 1.5-fold cardiac S1 to the actin solution. Light scattering was measured when values reached a plateau level in 10−20 min. Stable bundles of actin filaments were formed at low ionic strength, whereas less was observed at higher ionic strength. (B) Dependence of bundle formation on S1-to-actin ratios. Light scattering of actin solution was monitored in the presence (open triangles) and absence (open circles) of 200 mM NaCl. The light scattering of actin solution containing 200 mM NaCl was subtracted from that containing no NaCl to estimate the amount of actin bundle formation (closed circles) as increasing the amount of S1 as indicated on the abscissa. The bundle formation thus estimated was approximately a quadratic function of the S1-to-actin ratio (broken line) until the ratio reached 1 (formation of fully S1 decorated actin filament).

the bundle formation is saturated at the 1:1 S1:actin ratio.

Protein interaction was examined by zero-length cross-linking experiments after bundles had formed. This experiment was aimed to identify any band which appeared when bundles were formed with knowledge of previous studies (*20*−*25*). Addition of cardiac S1 to an actin solution resulted in bundle formation at 0 mM NaCl and observed cross-linking between actin and cardiac ELC (64 kDa band), and also between actin, cardiac S1 heavy chain, and cardiac ELC (at about 158 and 200 kDa) (Figure 4a−e). When actin

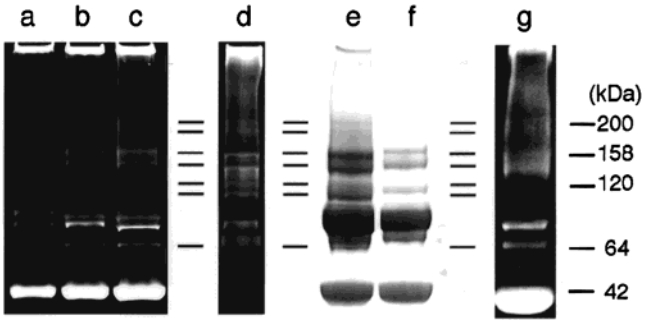

FIGURE 4: SDS−PAGE analysis of cross-linked bundles. Actin filaments labeled with 1 μM DACM were mixed with 0, 0.5, and 1 μM cardiac S1 (a, b, and c) and cross-linked with EDC as described under Experimental Procedures. IAF-labeled cardiac ELC was incorporated into cardiac S1 and cross-linked with actin by EDC (d), when bundles were formed. Coomassie staining was obtained for 1.5 μM cardiac S1 and 1 μM actin cross-linked with EDC at 0 mM NaCl (e) and at 200 mM NaCl (f). MBS-treated DACM actin was added to actin bundles formed by cardiac S1 and cross-linked by EDC (g). Bars indicate molecular mass corresponding to around 64 kDa ELC 1−actin (bottom), around 158 kDa actin−S1 heavy chain−ELC 1 (middle two), and around 200 kDa actin−S1 heavy chain−ELC 1−actin (top two), according to the amino acid sequence reported by Nakayama et al. (*40*) and Maita et al. (*10*). The reason two bands for the same chain mass product were seen might be due to cross-linking occurring at multiple points between proteins.

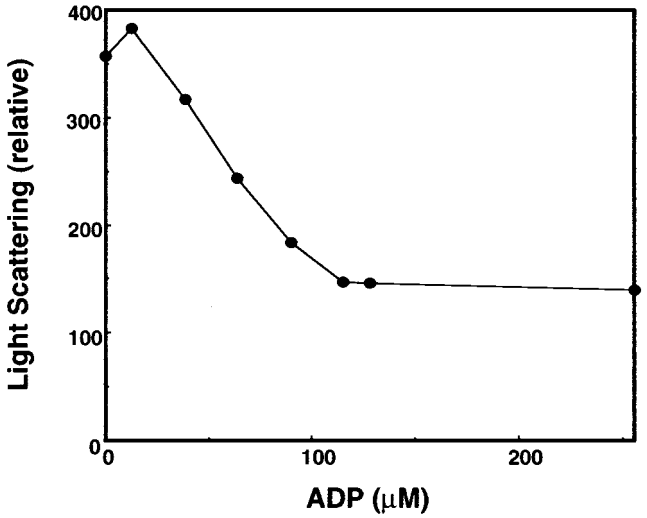

FIGURE 5: Effect of ADP on the formation of actin bundles monitored by light scattering. Actin filament bundles were formed as described for Figure 1 and mixed with 0−256 μM ADP. ADP decreased the light scattering down to one-third of the maximum, and 5×10^{-5} M ADP was for its half-change.

bundle formation was absent in the presence of 200 mM NaCl, formation of actin−cardiac ELC cross-linking (64 kDa band) was significantly suppressed, whereas actin−cardiac S1 heavy-chain−cardiac ELC cross-linking (158 kDa band) continued to be clearly observed (Figure 4f). When a 10-fold molar excess of fluorescently labeled MBS-actin was added to actin moiety bundled with cardiac S1, the 64, 158, and 200 kDa bands also continued to be observed (Figure 4g), as will be discussed later.

ADP was reported to make structural changes in the S1 tail portion relative to its tip or head portion (*14*, *26*). We examined the effect of ADP on actin bundling. As shown by the change in light scattering (Figure 5), ADP was an effective analogue of ATP in breaking up actin bundles. This

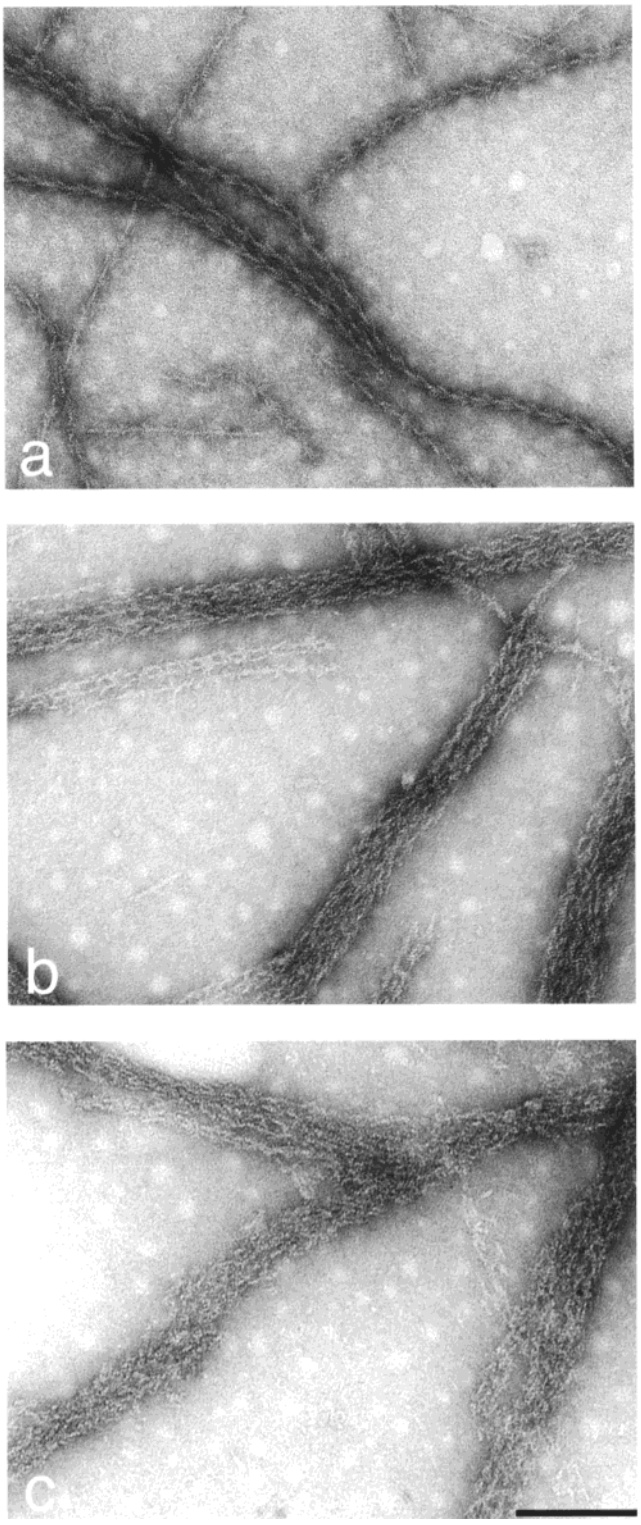

FIGURE 6: Electron micrographs of actin bundles in the presence of ADP. Actin bundles formed were dispersed by adding 100 μM ADP (a). Among single actin filaments, many incompletely bundled actin filaments were seen mostly with a parallel arrowhead pattern in the presence of ADP. More than two actin filaments were often bundled so as to form sheets when cross-linked with EDC, as seen in (b). Such sheets of actin bundles were scrambled by adding 100 μM ADP (c). Bar indicates 0.2 μm.

effect of ADP was confirmed by electron microscopy of an actin bundle solution in the presence of 100 μM (Mg^{2+}) ADP (Figure 6a). ADP addition decreased the number of actin bundles, and more of the remaining actin bundles were

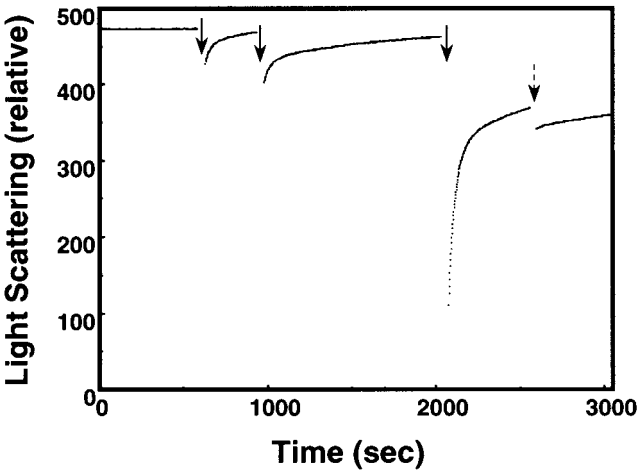

FIGURE 7: Actin bundles dispersed transiently by adding an excess amount of monomeric actin molecules. Actin filaments (1 μM actin) bundled by addition of 1.5 μM cardiac S1 were mixed twice with 1 μM monomeric actin at the time indicated by the first and the second arrows. The resultant mixture was further added with 8 μM monomeric actin at a time indicated by the third arrow. Significant reduction of light scattering was observed. A part of the mixture was put on the grid and quickly frozen for electron cryo-microscopy at the time indicated by the fourth dotted arrow.

arrayed in parallel. EDC cross-linking of actin bundles with cardiac S1 made actin bundle sheets as shown in Figure 6b. ADP, however, scrambled the EDC cross-linked bundles (Figure 6c). AMPPNP as well as ADP induced similarly a decrease of the light scattering from a solution of actin bundles (data not shown).

It was previously reported that the orientation of the Cys 707 ("SH1") residue of myosin heavy chain could change by adding ADP in a muscle fiber while that of the Cys 697 ("SH2") residue remained unchanged, indicating that ADP induced a relative movement around the residues (*14*, *27*). We examined further whether ADP may induce such possible movement in this region of cardiac myosin. Rhodamine dye attached to the SH1 of cardiac S1 was used as a probe for detecting movement of the SH1 portion of S1 upon addition of ADP. The rhodamine dipole was estimated to lie at about 60° relative to the axis of actin filaments (or of the muscle fiber) and to reorient at about 30° in the presence of 100 μM ADP. This result is consistent with a previous observation using rabbit skeletal myosin S1 (*14*, *27*).

The spacing between actin filaments in an actin bundle (20 nm) suggests direct binding of the S1 tail to the adjacent actin filament. In this case, the extra binding site can be blocked by actin monomers. To examine this hypothesis, we added actin monomers to a solution containing actin bundles. MBS-actin was used as actin monomer in the experiment (Figure 7). After actin bundles were formed by cardiac S1, 1 μM MBS-actin was added twice to the solution containing 1 μM actin and 1.5 μM cardiac S1, and later 8 μM MBS-actin was added to ensure binding of monomeric actin. Significant reduction of the light scattering was observed (Figure 7); the same sample was then quickly frozen at liquid ethane temperature, and was observed by electron cryo-microscopy (Figure 8). Many single actin filaments with arrowheads were observed among the disassembled bundles (Figure 8), suggesting that actin monomer was able to disperse actin filaments from their bundles. As a control, the effect of BSA, an inert protein, was examined by light

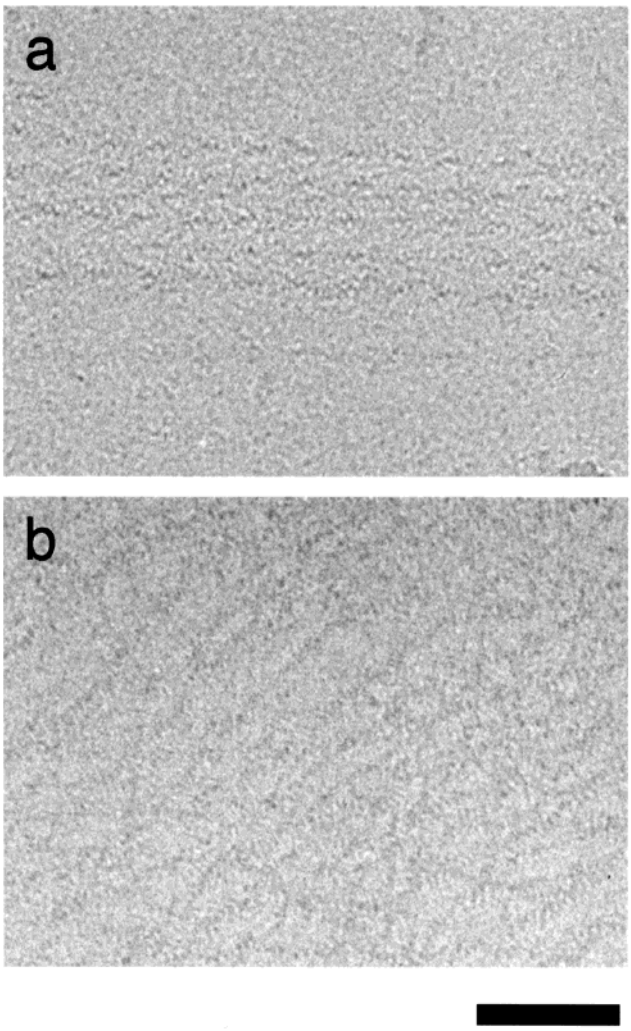

FIGURE 8: (a) Electron cryo-micrographs of actin bundles after mixing with monomeric actin. Bundle formation of actin filaments was induced by cardiac S1 (see Figures 1 and 2). (b) Monomeric MBS-actin was added to the actin bundle solution and sampled as described for Figure 7. Actin bundles became disassembled into single filaments. Bar indicates 0.1 μm.

scattering and found to be ineffective (data not shown).

MBS-treated actin may possibly be cross-linked to dimer in addition to the majority of monomer molecules. Skeletal myosin head can be cross-linked with a dimer of MBS-actin (*28*). Polymerization of MBS-actin solution was detected by viscosity when its concentration was on the order of milligrams per milliliter (*29*). The fluorescent probing method used here may be sensitive to detect such a possibility as we found a band which may correspond to the size of actin dimer (Figure 4g) whereas actin dimer was much evident in the cross-link experiment using regular actin (Figure 4a−c). Electron microscopy of such a sample did not show any evident actin dimer or actin filament without arrowhead (Figure 8b) under the same condition as used for Figure 4g, indicating that the amount of actin dimer was small if any.

Figure 9a shows a three-dimensional reconstruction of a single actin filament, which has been disassembled from a bundle by treatment with excess actin monomers. From comparing this with the three-dimensional reconstruction of a single actin filament in the absence of MBS-actin (Figure 9b), the protrusion that does not exist in Figure 9b could be seen in Figure 9a. The catalytic domain (residues 1−710 of the S1 heavy chain) including the ATPase- and actin-binding sites and the light-chain-binding domain (residues from 782 to the end of S1 heavy chain) including the ELC- and RLC-binding regions are separated in the middle part of the whole head—the "converter domain" (residues 711−781) (*30*). The extra density region (Figure 9a minus Figure 9b) due to adding MBS-actin to an acto−S1 filament could be clearly observed in the middle part of the S1 head (Figure 9c): When the three-dimensional image reconstructed from electron cryo-micrographs was fitted to the atomic model of actin−skeletal S1 complex (Figure 9d) (*31*), the extra density region corresponded to the converter domain and the ELC-binding region. The extra density region elongated from a part of ELC to around residues 739 and 762 of the S1 heavy chain. This density could be due to MBS-actin itself or to the S1 tail domain whose structure has been changed by binding of MBS-actin. In either case, it is likely that MBS-actin interacted with the middle part of the whole head near the ELC-binding region of S1. The distance between the actin-binding site (around residue 640 of the heavy chain) and the binding site of MBS-actin within one head could be estimated to be about 9 nm according to the three-dimensional reconstruction used for Figure 9.

A three-dimensional reconstruction of acto−cardiac S1 (without MBS-actin, Figure 9b) does fit well with the atomic model of acto−S1 based on X-ray models of acto−skeletal S1, from the catalytic domain to part of the ELC-binding region. At the rest of the ELC-binding region and the RLC-binding region in the light-chain-binding domain, the three-dimensional reconstructions of myosin heads are slightly distinguishable from each other for the acto−cardiac S1 and the acto−skeletal S1 complexes. Since the reconstruction from electron cryo-microscopy of acto−skeletal S1 fits well to the atomic model (Figure 9d) (*31*), the S1 in acto−cardiac S1 may slightly bend at its tail end region.

DISCUSSION

"Bundling" of actin filaments in the presence of skeletal myosin head was first reported by Ando (*5*), and was further investigated by us (*6*), showing that the bundle-forming capability of the myosin head depends on the ELC isoform in fast skeletal muscle. A cluster of basic amino acid residues of ELC 1 at the amino-terminal portion of its extended polypeptide chains, compared to ELC 2, was found to be important for interaction of the myosin head with an actin molecule (*2*, *4*, *32*). In the present study, this feature was found especially evident in cardiac myosin head. Here we look into the mechanism of bundle formation and examine characteristic features of myosin head from cardiac muscle.

Cardiac S1 with ELC obtained by chymotryptic digestion of myosin filaments is peculiar in its speed of actin bundle formation. As soon as the actin solution was mixed with a slight molar excess of cardiac S1, bundle formation started (Figure 1). The rate-limiting process in this experiment was actually the mixing process. The initial rate of bundle formation by cardiac S1 was too fast to be determined by manual mixing. The time for reaching the half-maximum of light scattering increase by bundle formation was estimated to be about 5 s for cardiac S1, whereas that for skeletal S1 with cardiac ELC or for skeletal S1 with skeletal ELC 1 was significantly slower as described previously. The

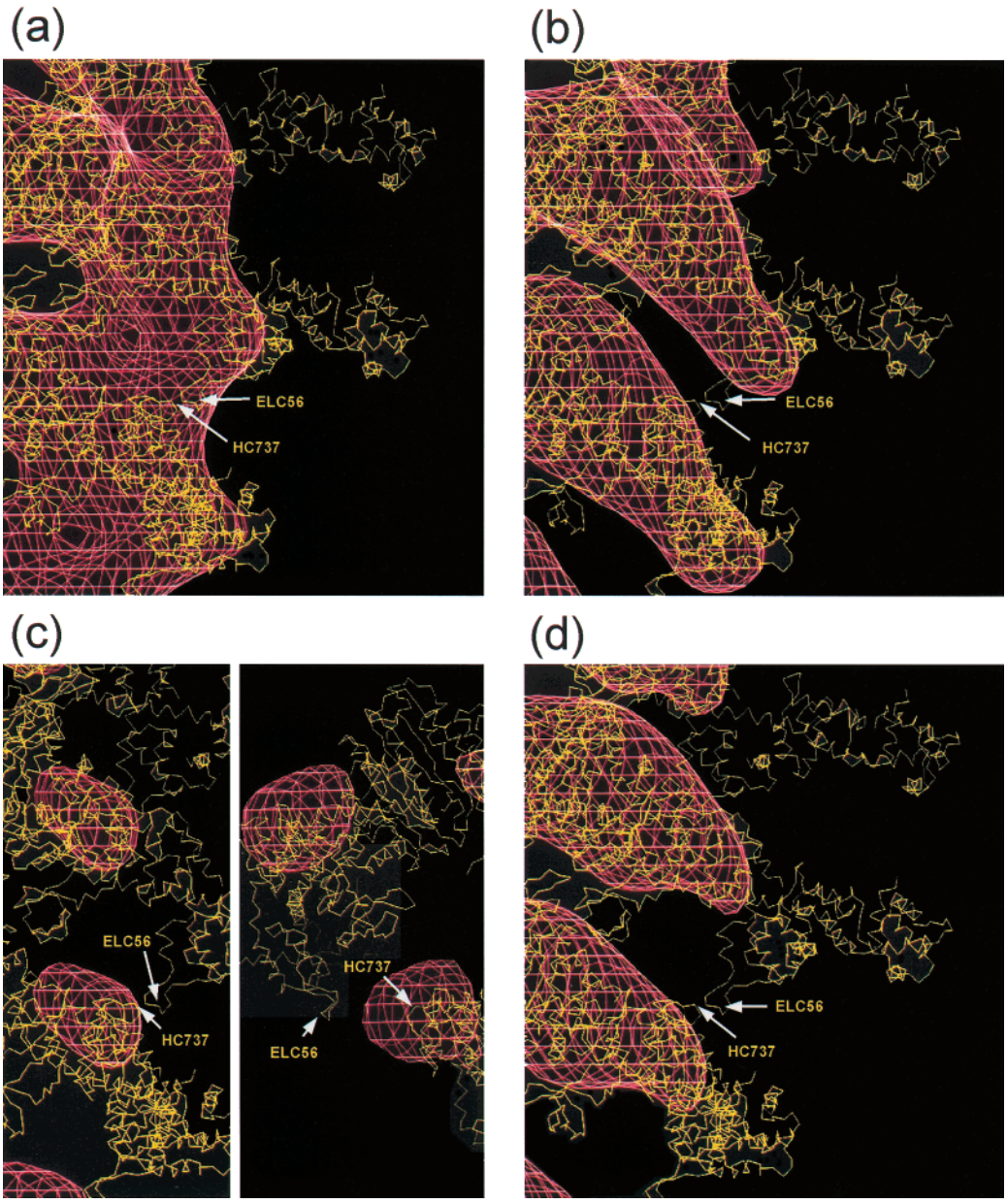

FIGURE 9: Three-dimensional image reconstructed from electron cryo-micrographs of single actin filaments in the presence or absence of excess monomeric actin. (a) Three-dimensional reconstitution image of single actin filaments, which have been dispersed from the bundle by excess monomeric MBS-actin (Figure 8b). The protrusion could be seen in the middle part of the myosin head which resides between residue 740 of the heavy chain and the ELC-binding region as described under Results. The three-dimensional image in red was compared with an atomic model of actin−skeletal S1 in gold (*31*). (b) Three-dimensional image reconstructed from single actin filaments in the absence of MBS-actin. (c) Difference map by subtracting the densities of the map without MBS-actin from that with MBS-actin. The extra density region was observed and colored in red. Two profiles of the same difference map are shown, and the left one is viewed from the same angle as used in (a), (b), and (d). The two arrows in (a), (b), and (c) indicate HC737 and ELC56, respectively. (d) Three-dimensional image of actin−skeletal S1 complex as a reference map (*31*). In comparison with the three-dimensional images of actin−cardiac S1 complex without MBS-actin (b), the light-chain-binding domain of cardiac S1 slightly bends.

combination of cardiac heavy chain and cardiac ELC seemed to be most effective in forming bundles of actin filaments. A part of cardiac myosin heavy chain may be involved in the bundling capability. When we compare the amino acid sequences of atrial, ventricle, and skeletal myosin heavy chains according to Geeves and Holms (*30*), there are marked differences among the three at the amino-terminal/SH3-like β-barrel structure, loop 1, loop 2, and the light-chain-binding regions and some difference at the converter domain (Figure 10). Those differences in the primary structure, especially the actin-binding (loop 2) and the light-chain-binding domains, may partly account for the functional differentiation in cardiac and skeletal myosins. We observed a characteristic bending in the three-dimensional structure around the light-chain-binding domain for ventricle myosin S1, as described for Figure 9b under Results. The region related to ATP binding and hydrolysis seems conserved.

Electron microscopy of actin bundles showed that bundles with cardiac S1 were not much different from bundles with skeletal S1 (*5*, *6*). The two adjacent actin filaments were usually antiparallel arrowheaded with a center-to-center distance of about 20 nm and with cross-attachments of about 35 nm intervals along the filament axis. Since the actin monomer has about a 5.5 nm radius, the space between the

FIGURE 10: Comparison of the amino acid sequences of S1 moieties of chicken pectoralis myosin heavy chain (MYSS_CHICK), ventricle myosin heavy chain (JX0317, BAA92710), and atrial myosin heavy chain (BAB47399). The common amino acid residue among the three myosins is shown by an asterisk under the amino acid lines, the common between the two is shown by a dot, and no common amino acid residue among the three is marked by an open space. Notes, i.e., SH3, P-loop, loop 1, SW I, 50 kD link, SW II helix, loop, loop 2, converter, ELC binding, RLC binding, are given according to Geeves and Holms (*30*).

two filaments is about 9 nm, which is close to the length of the catalytic domain in the myosin head. Therefore, a bundle is hardly made from the tail-to-tail interaction of myosin heads attached to actin filaments. Full decoration of actin filaments with S1 was required for bundle formation (Figure 3B). This suggests that the S1 tail portion in the fully decorated actin filaments may have to protrude to interact with the adjacent actin filament.

The actin bundles could be dispersed by increasing the salt concentration, and bundle formation was suppressed under the high-salt conditions (Figure 2b,c and Figure 3). Bundle formation was pH-dependent. These lines of evidence suggest that some ionic interaction between the fully S1 decorated actin filaments may be required for bundle formation. The amino-terminal portions of skeletal ELC 1 and cardiac ELC have a similar basic cluster of amino acid residues and may work as an antenna to watch for actin to bind (*2*, *4*, *6*, *10*, *32*).

In muscle fiber, since the S1:actin binding ratio is expected to be relatively low (less than 1), ELC may possibly bind easily to the same actin as the conventional actin-binding region of S1 binds (*21*). A cross-linked band of ELC 1−actin can be formed under such experimental conditions. As the ratio of S1 added to actin increased, actin binding through the ELC of cardiac S1 on an actin filament may be competitively chased away from the filament by the stronger conventional actin binding of the other S1 so that there is less ELC/actin cross-linking (*20*, *22*). However, this may cause ELC to search for other possible actin binding and can reach out to a part of an actin molecule in the other actin filament under the present experimental conditions. We could replace the bound actin through the ELC region of cardiac S1 between actin filaments in the bundle, with externally added monomer actin molecules, should they be available in the solution, which may allow the monomer actins to bind regularly the outer region of S1 in the arrowheaded structure of acto−cardiac S1 filament.

When MBS-actin at a molar ratio in a slight excess of the S1 moiety was added to cardiac S1 actin bundles, dispersion of bundles was not evident. However, adding about 10 times molar excess of MBS-actin to the S1 moiety clearly dispersed actin bundles, and recovery of actin bundles was slow or was lessened (Figure 7), as observed by cryo-electron microscopy (Figure 8a,b). Under the same conditions, MBS-actin monomer with a fluorescent probe could be cross-linked to ELC and the heavy chain of cardiac S1 (Figure 4g). Comparing the three-dimensional reconstruction of a single actin filament in the presence of MBS-actin with that in the absence of MBS-actin, the extra density region was observed in the former. This extra density region was considered to be due to the presence of MBS-actin. All the results obtained above were consistent with the idea that cardiac S1 can interact with an actin molecule at the region in the vicinity of its ELC-binding domain, while it can also tightly bind to actin filament at the conventional actin-binding region near the so-called loop 2 in the myosin head moiety (*30*, *33*). In fact, the extra density region due to the binding of MBS-actin was found between the ELC-binding region and the converter domain, when the difference map (Figure 9a minus Figure 9b) was compared with the atomic model of the acto−S1 complex by Mendelson and Morris (*31*) (Figure 9c). The converter domain was suggested to be located in residues 711−781 of the myosin heavy chain (*30*, *34*). In the present study, therefore, cardiac myosin heads are proposed to interact with actin molecule at two regions: one region including the conventional loop 2 portion and another region

between the converter and the ELC-binding domains as the second actin-binding region. Recently Pliszka et al. showed that the amino-terminal part of ELC 1 of skeletal myosin may localize in the vicinity of the converter domain (*35*).

Arata reported that MBS-actin could bind myosin filament with a dissociation constant of 3×10^{-6} M for monomer actin and 3×10^{-7} M for dimer actin (*23*). Bettache et al. reported that the dissociation constant was $(0.2-0.5) \times 10^{-6}$ M for the monomer actin−skeletal myosin S1 complex at low ionic strength (*29*). In this study, we have not determined the association constant of cardiac S1 to MBS-actin. However, the experimental results that 1−2 μM MBS-actin could slightly disassemble 1 μM actin filament in the bundle and that 10 μM MBS-actin disassembled more than the half of the original amount of bundled actin filaments into many single filaments (Figures 7 and 8b) may be compatible with the idea that MBS-actin used here may bind cardiac S1 at its second actin-binding region with a dissociation constant of the order of 10^{-6} M but not in the range of that for conventional actin binding ($10^{-8}-10^{-9}$ M) (*36*).

The interactions between ELC and actin; between S1 heavy chain, ELC, and actin; and between S1 heavy chain, ELC, and two actin molecules existed, but no interaction between S1 heavy chains was discerned (Figure 4a−f). The difference between when bundles were formed at low ionic strength and when no bundle was formed at high ionic strength was primarily the formation of the 64 kDa, ELC−actin, band (Figure 4e,f). The minor 200 kDa band corresponding to the combination of two actins and cardiac HC and ELC was also more detectable at low ionic strength when bundles were formed. These results suggest that the ELC-binding region of cardiac S1 on an actin filament can bind an actin molecule in the adjacent actin filament in the bundle, being consistent with the spacing between actin filaments in bundles and with the proposed interaction between actin and ELC.

ADP is thought to make structural changes in the S1 tail portion relative to its tip or head portion (*14*, *26*). Formation of the ADP−acto−S1 ternary complex may be effective in altering the formation of actin bundles (Figure 5), as observed by electron microscopy (Figure 6a). Actin bundles made firm by EDC cross-linking were also disrupted by addition of ADP (Figure 6b,c). ADP binding to the acto−cardiac S1 complex can be estimated with the association constant in a range of 10^5 M^{-1} (Figure 5). This is consistent with the previous report that ADP bound to the acto−cardiac S1 complex with an association constant of 1.5×10^5 M^{-1} to form a ternary complex (*36*). ADP changed the orientation of the cardiac S1 tail portion in muscle fiber similar to the effect of ADP on the skeletal S1 tail portion, as described under Results (*14*, *27*). The actin filaments with cardiac S1 in the bundles showed a different (parallel arrowhead) pattern in the presence of ADP (Figure 6a) than that in its absence (antiparallel) (Figure 2a). These lines of observations suggest that the manner of cardiac S1 interacting with another actin molecule at the converter−ELC 1 region may depend on the presence and type of nucleotide while it binds actin molecule at the conventional actin-binding region.

Cardiac S1 dissociated from actin filament in the presence of ATP slower than rabbit skeletal S1 (*37*). The rate of ADP release from A−M·ADP ("A" for actin and "M" for myosin) is sufficiently slow to limit the unloaded shortening velocity in cardiac muscle (*36*). Slow breakdown of A−M·ADP may account for maintaining tension with a low ATP turnover rate (*38*). ADP may reduce the rate of crossbridge detachment, resulting in a decreased ATP consumption and an increased economy of force production under ischemic conditions in cardiac muscle (*39*). Slow decomposition of A−M·ADP as described for cardiac muscle may be related to specific structure, which can reinforce the binding of cardiac S1 with ADP to actin. In this work, we raised a feature for cardiac myosin binding actin molecule at two separate regions, its evidence arising from observing in vitro that chicken ventricle myosin forms stable actin bundles. The two actin-binding regions may also work together when the S1:actin ratio is lower than the experimental conditions used for the present study, as expected in physiological conditions. ELC and actin can be cross-linked more at a low cardiac S1:actin ratio than at a high ratio (*22*), and such interaction could occur in skeletal myofibril (*21*). The tail portion of cardiac S1 might be forced to protrude to the surface of the arrowheaded actin filament when the S1:actin ratio is more than 1, as observed under Results (Figure 9b), and actin bundles as a sign of the "acting" second actin-binding region of myosin head can be formed. In the presence of ADP forming the ternary complex with acto−cardiac S1, we can still observe such a bundle in a slightly different manner than its absence. These observations may support the idea that the second actin-binding region of cardiac S1 possibly helps the S1 with ADP to bind actin long enough to give a low tension cost for cardiac muscle contraction.

ACKNOWLEDGMENT

We thank Dr. Manuel F. Morales (University of the Pacific, San Francisco, CA) for his critical reading of the manuscript. We are grateful to Dr. Toshiaki Arata (Osaka University, Osaka, Japan) for his discussion about MBS-actin. One of the authors (T. Miyanishi) is grateful for his encouragement of Dr. Mitsuji Inoue (Shunkaikai Medical Foundation, Nagasaki, Japan).

NOTE ADDED AFTER ASAP POSTING

The author byline was changed and present addresses were added for T. I and T. W. The correct version was posted 4/23/02.

REFERENCES

1. Matsuda, G. (1983) *Adv. Biophys. 16*, 185−218.
2. Hayashibara, T., and Miyanishi, T. (1994) *Biochemistry 33*, 12821−12827.
3. Lowey, S., Waller, G. S., and Trybus, K. M. (1993) *J. Biol. Chem. 268*, 20414−20418.
4. Timson, D. J., Trayer, H. R., and Trayer, I. P. (1998) *Eur. J. Biochem. 255*, 654−662.
5. Ando, T. (1987) *J. Mol. Biol. 195*, 351−358.
6. Hayashibara, T., Miyanishi, T., and Maita, T. (1994) *Acta Med. Nagasaki 39*, 157−162.
7. Tonomura, Y., Appel, P., and Morales, M. (1966) *Biochemistry 5*, 515−521.
8. Murakami, U., Uchida, K., and Hiratsuka, T. (1976) *J. Biochem. (Tokyo) 80*, 611−619.
9. Weeds, A. G., and Taylor, R. S. (1975) *Nature 257*, 54−56.
10. Maita, T., Umegane, T., Kato, Y., and Matsuda, G. (1980) *Eur. J. Biochem. 107*, 565−575.
11. Wagner, P. D., and Stone, D. B. (1983) *J. Biol. Chem. 258*, 8876−8882.

12. Spudich, J. A., and Watt, S. (1971) *J. Biol. Chem. 246*, 4866−4871.
13. Laemmli, U. K. (1970) *Nature 227*, 680−685.
14. Miyanishi, T., and Borejdo, J. (1989) *Biochemistry 28*, 1287−1294.
15. Bettache, N., Bertrand, R., and Kassab, R. (1989) *Proc. Natl. Acad. Sci. U.S.A. 86*, 6028−6032.
16. Ishikawa, T., and Wakabayashi, T. (1999) *J. Biochem. (Tokyo) 126*, 200−211.
17. Dubochet, J., Adrian, M., Chang, J. J., Homo, J. C., Lepault, J., McDowall, A. W., and Schultz, P. (1988) *Q. Rev. Biophys. 21*, 129−228.
18. Crowther, R. A., Henderson, R., and Smith, J. M. (1996) *J. Struct. Biol. 116*, 9−16.
19. Amos, L. A., Henderson, R., and Unwin, P. N. (1982) *Prog. Biophys. Mol. Biol. 39*, 183−231.
20. Andreev, O. A., and Borejdo, J. (1995) *Biochemistry 34*, 14829−14833.
21. Andreev, O. A., and Borejdo, J. (1999) *Biochem. Biophys. Res. Commun. 258*, 628−631.
22. Andreev, O. A., and Borejdo, J. (1997) *Circ. Res. 81*, 688−693.
23. Arata, T. (1991) *J. Biochem. (Tokyo) 109*, 335−340.
24. Arata, T. (1996) *Biochemistry 35*, 16061−16068.
25. Bettache, N., Bertrand, R., and Kassab, R. (1992) *Biochemistry 31*, 389−395.
26. Whittaker, M., Wilson-Kubalek, E. M., Smith, J. E., Faust, L., Milligan, R. A., and Sweeney, H. L. (1995) *Nature 378*, 748−751.
27. Borejdo, J., Assulin, O., Ando, T., and Putnam, S. (1982) *J. Mol. Biol. 158*, 391−414.
28. Arata, T. (1998) *J. Struct. Biol. 123*, 8−16.
29. Bettache, N., Bertrand, R., and Kassab, R. (1990) *Biochemistry 29*, 9085−9091.
30. Geeves, M. A., and Homles, K. C. (1999) *Annu. Rev. Biochem. 68*, 687−728.
31. Mendelson, R., and Morris, E. P. (1997) *Proc. Natl. Acad. Sci. U.S.A. 94*, 8533−8538.
32. Morano, I. (1999) *J. Mol. Med. 77*, 544−555.
33. Sellers, J. R. (1999) *Myosins*, 2nd ed., Oxford University Press, New York.
34. Dominguez, R., Freyzon, Y., Trybus, K. M., and Cohen, C. (1998) *Cell 94*, 559−571.
35. Pliszka, B., Redowicz, M. J., and Stepkowski, D. (2001) *Biochem. Biophys. Res. Commun. 281*, 924−928.
36. Siemankowski, R. F., and White, H. D. (1984) *J. Biol. Chem. 259*, 5045−5053.
37. Taylor, R. S., and Weeds, A. G. (1976) *Biochem. J. 159*, 301−315.
38. Geeves, M. A. (1989) *Biochemistry 28*, 5864−5871.
39. Yamashita, H., Sata, M., Sugiura, S., Momomura, S., Serizawa, T., and Iizuka, M. (1994) *Circ. Res. 74*, 1027−1033.
40. Nakayama, S., Tanaka, H., Yajima, E., and Maita, T. (1994) *J. Biochem. (Tokyo) 115*, 909−926.

BI0118355